Star Polymers Confined in a Nanoslit: A Simulation Test of Scaling and Self-Consistent Field Theories

ARTICLE *in* SOFT MATTER · JULY 2013

Impact Factor: 4.03 · DOI: 10.1039/c3sm51275d · Source: arXiv

4 AUTHORS, INCLUDING:

Andrey Milchev
Bulgarian Academy of Sciences
237 PUBLICATIONS **4,464** CITATIONS
SEE PROFILE

Sergei Egorov
University of Virginia
91 PUBLICATIONS **1,956** CITATIONS
SEE PROFILE

Kurt Binder
Johannes Gutenberg-Universität Mainz
1,065 PUBLICATIONS **45,266** CITATIONS
SEE PROFILE

Macromolecules

Article

pubs.acs.org/Macromolecules

The Escape Transition of a Compressed Star Polymer: Self-Consistent Field Predictions Tested by Simulation

Jarosław Paturej,*[,†,‡] Andrey Milchev,[§,∥] Sergei A. Egorov,[⊥] and Kurt Binder[∥]

[†]Department of Chemistry, University of North Carolina, Chapel Hill, North Carolina 27599-3290, United States

[‡]Institute of Physics, University of Szczecin, Wielkopolska 15, 70451 Szczecin, Poland

[§]Institute of Physical Chemistry, Bulgarian Academy of Sciences, Sofia 1113, Bulgaria

[∥]Institut für Physik, Johannes Gutenberg Universität Mainz, Staudinger Weg 7, D-55099 Mainz, Germany

[⊥]Department of Chemistry, University of Virginia, Charlottesville, Virginia 22901, United States

ABSTRACT: The escape transition of a polymer "mushroom" (a flexible chain grafted to a flat nonadsorbing substrate surface in a good solvent) occurs when the polymer is compressed by a cylindrical piston of radius R, that by far exceeds the chain gyration radius. At this transition, the chain conformation abruptly changes from a two-dimensional self-avoiding walk of blobs (of diameter H, the height of the piston above the substrate) to a "flower conformation", i.e., stretched almost one-dimensional string of blobs (with end-to-end distance $\approx R$) and an "escaped" part of the chain, the "crown", outside the piston. The extension of this problem to the case of star polymers with f arms is considered, assuming that the center of the star is grafted to the substrate. The question is considered whether under compression the arms escape all together or whether there occurs an arm by arm escape under increasing compression. Both self-consistent field calculations and molecular dynamics simulations are found to favor the latter scenario.

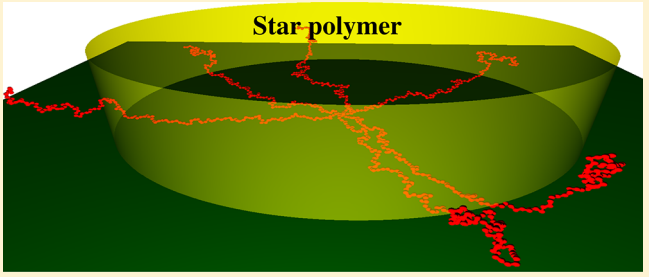

1. INTRODUCTION

During the past decades novel experimental techniques have been developed allowing the observation and manipulation of single chains grafted to (or adsorbed on) substrates.[1−16] A particular intriguing aspect is the response of such grafted polymers to stretching or compression forces (for excellent reviews of experimental work see e.g. ref 17 and for the theoretical aspects see ref 18). A particularly interesting phenomenon is that such single polymer manipulations may induce unconventional conformational transitions (see ref 18 and references therein). In the present work we shall focus on the so-called "escape transition".[19−32] Figure 1 shows a schematic sketch of the setup that is considered for the case of the escape of a single flexible macromolecule grafted to a planar nonadsorbing surface, as traditionally considered.[25] Such a polymer, under good solvent conditions, takes the so-called "mushroom configuration",[33] i.e., both components of the gyration radius parallel ($R_{g\|}$) and perpendicular ($R_{g\perp}$) of the chain scale with the number N of effective monomeric units as (cf. Figure 1)

$$R_{g\|} \propto R_{g\perp} \propto aN^{\nu} \tag{1}$$

where a is the linear dimension of an effective monomeric unit and ν is the "Flory exponent" $\nu = 3/5$ (or, more precisely, $\nu \approx 0.588$[33,34]). When the mushroom is compressed by a cylindrical piston of radius R (we consider only the idealized case that the axis of the piston is perpendicular to the surface, coincident with the z-axis through the grafting site) to a height H with $H \ll R_{g\perp}$ while $R \gg R_{g\|}$, one rather obtains a "pancake" conformation, i.e., a two-dimensional self-avoiding walk of "blobs" of diameter H.[33] For a number n of blobs, one has then

$$R_{g\|} = Hn^{3/4} \tag{2}$$

since in $d = 2$ dimensions the Flory exponent is $\nu_2 = 3/4$.[33] The standard scaling argument[35] implies that inside a blob one still has the same statistics as in the bulk ($d = 3$ dimensions), so $H = ag^{\nu}$ if there are g effective monomeric units per blob. Since thus $g = (H/a)^{1/\nu} \approx (H/a)^{5/3}$ and $n = N/g = N(H/a)^{-5/3}$, ignoring here and henceforth all prefactors of order unity in such scaling considerations, one obtains

$$R_{g\|} = N^{3/4}a(H/a)^{-1/4} \tag{3}$$

The free energy cost for creating this confinement is simply the thermal energy k_BT times the number of blobs

$$\Delta F(H)/k_BT = n = N(H/a)^{-5/3} \tag{4}$$

When the chain is escaped, one predicts instead a free energy cost independent of N[19,20]

$$\Delta F(H)/k_BT = R/H \tag{5}$$

Received: June 28, 2013
Revised: September 13, 2013

   dx.doi.org/10.1021/ma401356w | *Macromolecules* XXXX, XXX, XXX−XXX

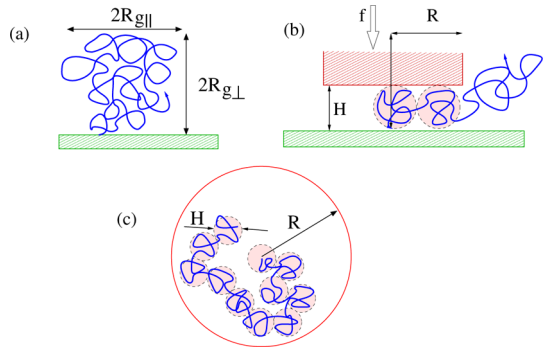

Figure 1. (a) Schematic plot of a "mushroom" (i.e., a chain grafted with one end at a flat repulsive wall). Linear dimensions of the coil parallel ($R_{g\|}$) and perpendicular ($R_{g\perp}$) to the substrate are indicated. Upon compressing the mushroom by a cylindrical piston of radius R axially centered at the grafting site, the chain forms "blobs" of diameter H, the height of the piston above the surface. Holding the piston at a chosen height H requires a force $\mathcal{F}$. The conformation of the chain may be "escaped" (part of the chain is not underneath the piston, case (b)) or "imprisoned" (the chain being fully underneath the piston, case (c)). While cases (a) and (b) refer to a side view, case (c) represents a top view.

Equating these two expressions yields a transition height

$$H_t/a = (Na/R)^{3/2} \tag{6}$$

and this transition is accompanied by a jump in the force $\mathcal{F} = -(\partial F/\partial H)_T$.

In the present paper, we shall be concerned with the escape transition when the macromolecule is not a simple linear chain but has a star polymer architecture.[36−40] In the limit where H is much smaller than the radius of a free star, the configuration of a star polymer with f arms confined into a slit of width H is essentially a quasi-two-dimensional star polymer, where each arm occupies a slice with an angle $2\pi/f$ cut from a cylinder of height H and radius $R_{\|}(f)$ with[41−44]

$$R_{\|}(f) = f^{1/4}(H/a)^{-1/4}N^{3/4} \tag{7}$$

The free energy in this case simply is[44]

$$\Delta F(H,f)/k_BT = fN(H/a)^{-5/3} \tag{8}$$

Comparing eqs 4−8, one simply notes that the free energy is additive in its contributions from the individual arms, which also have the same number n of blobs of diameter H as for a linear chain, in this limit of strong confinement.

When the star polymer is not compressed by a plate of infinite lateral extent but by a cylindrical piston of finite radius R, as in Figure 1, an escape transition for a star polymer also becomes conceivable, and the question that immediately comes to mind is will all arms escape at this transition, or will there be a sequence of f transitions, due to arm-by-arm escape? Sevick[45] suggested that the latter scenario applies, based on a simple Flory theory treatment.[33]

In the present work, we reconsider this problem, giving for the first time a more detailed self-consistent field treatment (section 2) and molecular dynamics simulations (section 3). Note that for finite chain length N the escape transition is not a sharp first-order transition but rather rounded by finite size effects,[25,26,32] and in view of multiple transitions located close by to each other, it is conceivable that the predicted singular behavior is completely washed out in cases of practical interest. Thus, it is important to study this problem beyond the simple level of Flory theory. Finally, section 4 presents discussion and concluding remarks. Note that molecular dynamics and self-consistent field methods are complementary: molecular dynamics is more accurate, taking all statistical fluctuations into account and, since it uses continuum models, is also more realistic. The self-consistent field method, however, which uses lattice formulation, implies mean-field approximations and hence is less accurate albeit it allows to treat much longer chains and stars with more arms, which is important for the present problem.

2. SELF-CONSISTENT FIELD THEORY

As is well-known, the self-consistent field (SCF) approach[46] takes excluded volume interaction into account only via a mean field approximation, like Flory theory[33] does, but unlike the latter it considers explicitly the nonuniformity of the monomer density distributions and deals with effects due to finite chain length: as is necessary for the present problem. Using the lattice

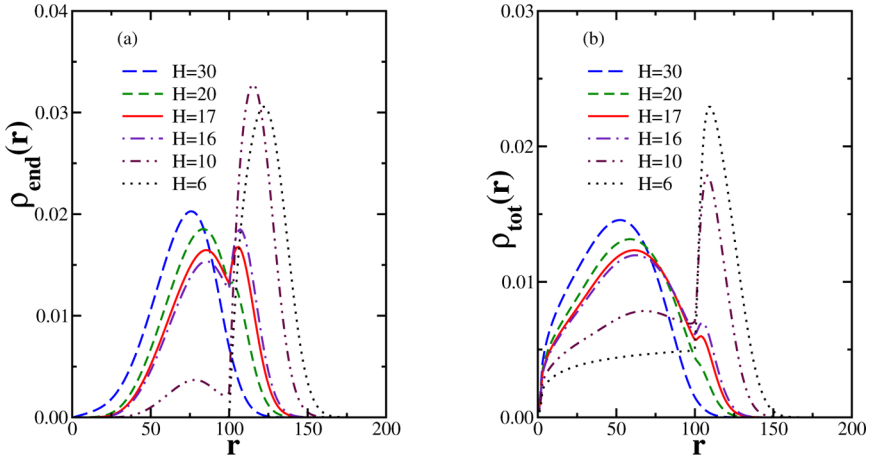

Figure 2. (a) SCF results for the radial density profiles $\rho_{end}(r)$ of the end segments in a star polymer grafted with its core at $r = 0$, $z = 0$, for the case $f = 10$, $N = 1000$, $R = 100$, and six different piston heights $H = 6$, 10, 16, 17, 20, and 30, as indicated. All lengths are measured in units of the lattice spacing a. (b) Same as (a) but for the radial density profiles $\rho_{tot}(r)$ of all segments. Note that both distributions are normalized to unity according to $\int \rho_{end}(r)\, dr = \int \rho_{tot}(r)\, dr = 1$ and thus incorporate a weighting factor $2\pi r$ already in their definition.

dx.doi.org/10.1021/ma401356w | Macromolecules XXXX, XXX, XXX−XXX

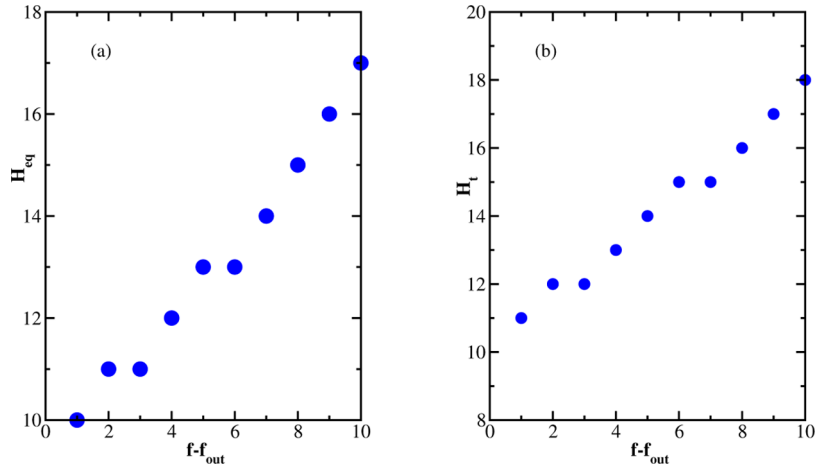

Figure 3. (a) SCF results for $H_{eq}(f_{out})$, the piston height at which the two peaks of $\rho_{end}(r)$ in Figure 2 have equal heights, versus $(f - f_{out})$, where f is the total number of arms and f_{out} is the number of arms that are constrained to have their end segments out of the piston. (b) Height H_t at which the escape transition of the first arm (from a fully "imprisoned" state of confinement) occurs plotted vs $f - f_{out}$; dots are from the locations of the "jumps" in Figure 5c.

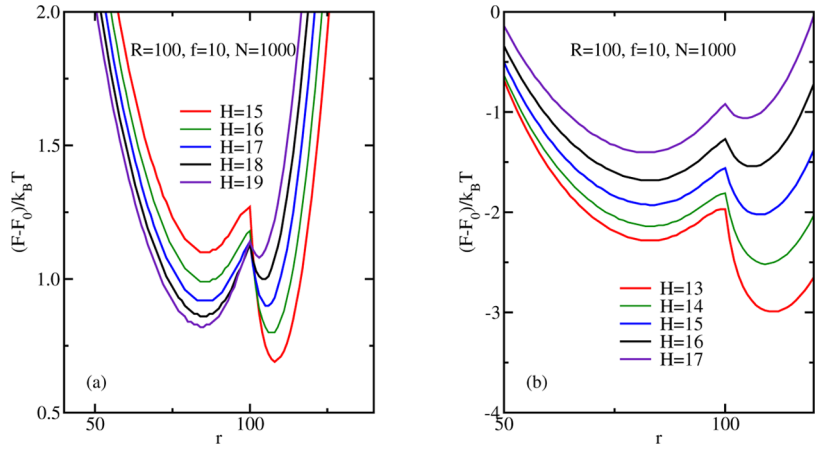

Figure 4. (a) Free energy function $F(r)$ relative to its reference value F_0 for the star polymer plotted as a function of the position r of the end monomer of one arm having its end monomer constrained to be at a radial distance r from the axis. Five different heights H = 15, 16, 17, 18, and 19 are included, as indicated. All data refer to the choice R = 100, f = 10, and N = 1000. (b) Same as (a), but with 3 arms escaped. Only choices of H near the transition value H are shown, namely H = 13, 14, 15, 16, and 17.

discretization as developed by Fleer et al.,[46] one can derive SCF equations for the volume fraction profiles of all monomeric species, putting the effective segment size a equal to the lattice spacing (which is our unit of length in this section). The SCF equations are nonlinear and need to be solved numerically by an iteration procedure. For this purpose, it is advantageous to take the symmetry of the problem into account. (In the present case, one can invoke a cylindrical symmetry around the axis of the cylindrical piston and formulate the problem in cylindrical coordinates, as described in ref 47 in another context.) Grafting is achieved by pinning an end-segment of each arm of the star to the core. Technical details of the method were described in the literature in detail[44,47] and hence will not be repeated here.

We consider a star polymer with f = 10 arms of length N = 1000 tethered by its core segment to a flat surface. In a first step, we compressed this star polymer by a cylindrical piston of radius R = 100. In Figure 2a, we show results for the radial density profiles of the free chain ends of the arms (not distinguishing yet to which arm the ends belong). One sees that for H = 30 and H = 20 the distribution has a single peak at $r = r_{max}^{(1)} < R$; as H decreases r_{max} increases, as expected. For H = 16 and H = 17 a double-peak structure with two peaks at $r_{max}^{(1)} < R$, $r_{max}^{(2)} > R$ of comparable height is seen, while for H = 10 and H = 6 the peak at $r_{max}^{(2)}$ clearly dominates. Thus, these results give clear qualitative evidence that for the chosen parameters an escape transition of star polymers can be observed. In Figure 2b, we show results for the radial density profiles of all the monomers of the star for the same six values of the piston height as in Figure 2a.

In order to turn to the issue of the arm-by-arm escape predicted by the Flory theory,[45] we have adopted the following strategy. We sequentially constrain f_{out} = 1, 2, 3, ... star arms to the end segment outside of the piston and determine the corresponding piston height $H_{eq}(f_{out})$ where the two peaks in the end segment distribution have equal heights. In the left panel of Figure 3 we plot $H_{eq}(f_{out})$ versus $f - f_{out}$. One sees that $H_{eq}(f_{out})$ shows a monotonic decrease with increasing f_{out}, which may be taken as an indirect evidence for arm-by-arm escape.

While it is known that the absolute values for the free energy of polymers predicted by the SCF theory often are unreliable,[44] we nevertheless expect that constructing a Landau free energy

dx.doi.org/10.1021/ma401356w | Macromolecules XXXX, XXX, XXX−XXX

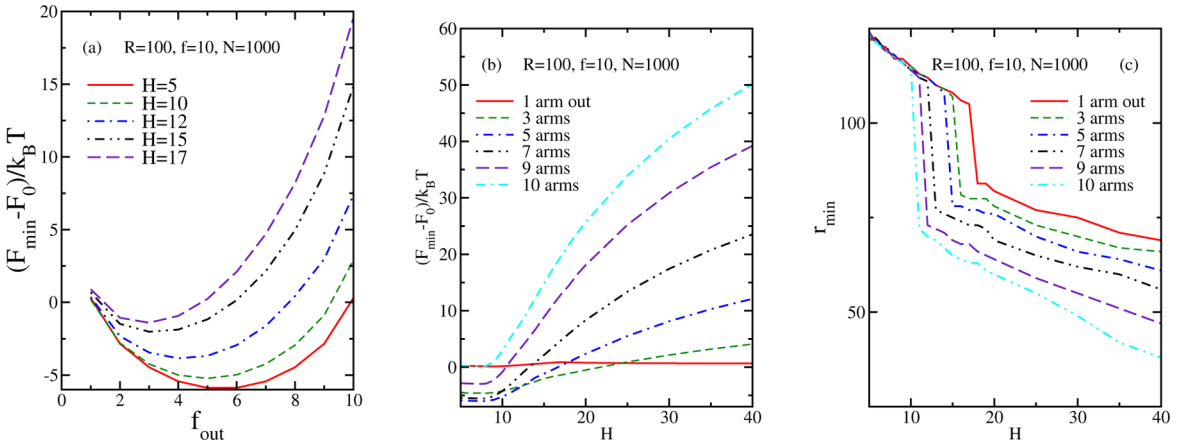

Figure 5. Free energy in its minimum F_{min} (cf. Figure 4) relative to the reference value F_0 for stars with $f = 10$ arms of length $N = 1000$, plotted versus the number f_{out} of arms constrained to be escaped, for different choices of H (a), and alternatively plotted as a function of H, for different choices of f_{out} (b). The lowest branches (in between the crossing points) clarify the range for which every value of f_{out} yields the stable state, while branches with higher free energy are metastable. Part (c) shows the variation of the minimum position r_{min} of F_{min}, for several choices of f_{out}, as indicated.

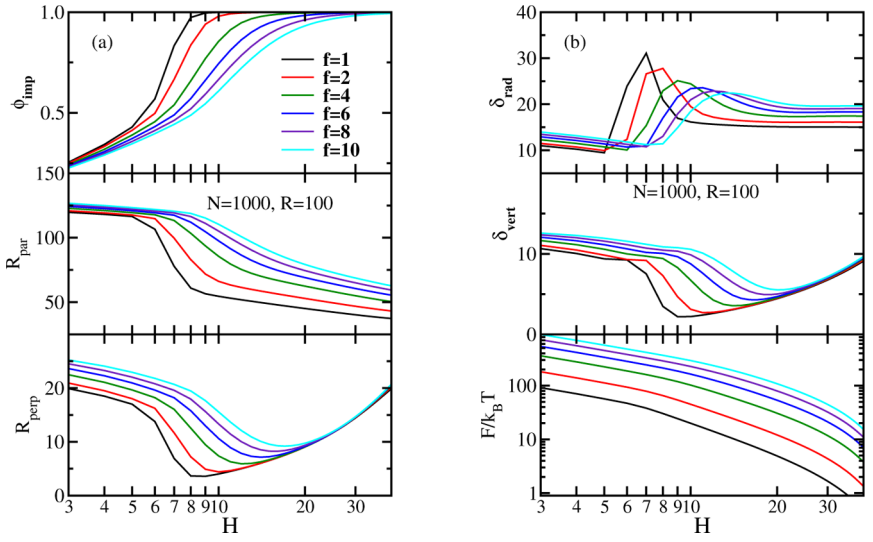

Figure 6. (a) Fraction of imprisoned monomers, ϕ_{imp} (upper panel), and parallel, $R_{g\|}$ (middle panel), as well as perpendicular, $R_{g\perp}$ (lower panel), gyration radius component of the grafted star polymer, plotted vs the piston height H. Various numbers of arms f are included, as indicated; all data are for the case $R = 100$, $N = 1000$. (b) Fluctuations of the free end-monomer in the radial, δ_{rad} (upper panel), and vertical, δ_{vert} (middle panel), directions. Lower panel: dimensionless compression free energy, F/k_BT, as a function of the piston height. The total free energy has a smooth, nonsingular variation, due to the rounding of the transition.

function similar to the spirit of the study of the escape transition of single chains[32] will give a useful first orientation (Figure 4a). Indeed, we see that $F(H,r)$ as a function of the position r of one constrained end-monomer develops a double well structure, with a barrier occurring at $r = R$; the scale of this barrier is only of order unity, however. Similar low barriers were also found for the escape transition of linear chains.[32] Thus, Figures 3 and 4a imply that although we expect that indeed arm-by-arm escape will occur in the thermodynamic limit (note that $N \to \infty$ and $R \to \infty$ must be taken together, keeping the ratio Na/R fixed, cf. eq 6, to obtain a sharp phase transition characterized by a truly singular behavior), for star polymers with physically realistic choices of parameters the transitions must be strongly rounded, and states with $f_{out} = 1, 2, 3, \ldots$ escaped arms have strongly overlapping distributions of all the observable properties. Along these lines, Figure 4b compares the free energy of the imprisoned and escaped stars for different choices of H in the vicinity of the transition at H_t, where one arm escapes, while two other arms are constrained to have their end-segment anywhere outside of the piston.

Next we consider the variation of the free energy with the number of arms constrained to be outside the piston, f_{out} (Figure 5). Plotting it versus f_{out} for different values of H (Figure 5a), we recognize that e.g. for $H = 17$ and $H = 15$ this minimum occurs at $f_{out} = 3$, while for $H = 12$ it occurs for $f_{out} = 4$, for $H = 10$ for $f_{out} = 5$, and for $H = 5$ for $f_{out} = 6$. In Figure 5b, the results are plotted alternatively as a function of H, for different choices of f_{out}. The lowest branches (in between the crossing points) clarify the range for which every value of f_{out} yields the stable state, while branches with higher free energy are metastable. Finally, Figure 5c shows the variation of the minimum position r_{min} of F_{min}, for several choices of f_{out}, as indicated. From the locations of the "jumps" in Figure 5c, one can determine the height H_t at which the escape transition of

dx.doi.org/10.1021/ma401356w | Macromolecules XXXX, XXX, XXX−XXX

the first arm (from a fully "imprisoned" state of confinement) occurs. This height is plotted vs $f - f_{out}$ as dots in the right panel of Figure 3, which shows behavior qualitatively similar to the one seen in the left panel of the same figure.

In Figure 6 we present SCF results for several structural and thermodynamic properties of compressed stars as a function of the piston height H, while the number of arms f is varied from 1 (linear chain) up to 10; in all cases the arm length is $N = 1000$, and the piston radius is $R = 100$. In particular, the upper panel of Figure 6a shows the variation with the piston height H of the "order parameter" (the fraction of imprisoned monomers, ϕ_{imp}), while middle and lower panels present the parallel and perpendicular gyration radius component of the star, respectively. From the upper panel, one sees that the transition is sharpest for the single chain ($f = 1$) and becomes more and more blurred as the number of arms increases. Note the nonmonotonic increase of $R_{g\perp}$ for small H: this reflects the contribution from the blob outside of the piston (Figure 1) which increases in size as H decreases.

The upper and middle panels of Figure 6b present the free end-monomer fluctuations in the radial and vertical directions, respectively. One sees that the fluctuations in the radial direction display a pronounced maximum as a function of the piston height H, whose height and sharpness both decrease with increasing number of arms, while its location moves to larger values of H, as one would expect. By contrast, fluctuations in the vertical direction show a minimum as a function of H, which is presumably related to the minimum observed in the vertical (perpendicular) component of the gyration radius of the grafted star polymer. The lower panel of Figure 6b shows compression free energy as a function of the piston height; it has a smooth, nonsingular variation, due to the rounding of the transition.

Referring back to Figure 4, we also note that the barrier between the two minima, separating the state with all arms being still confined (the left minimum) and the first arm being already escaped (the right minimum) decreases with increasing number of arms, and at the same time, the height H_t at which this transition occurs increases (right panel of Figure 3). This behavior is qualitatively easy to understand: the radius $R_{\|}(f)$ of a fully confined star increases with f (eq 7). On the other hand, it is not straightforward to predict this behavior from the theory: one could argue that the free energy of a compressed star with f arms is simply additive with respect to the contributions of the f arms. If we would assume that this is still true when one of the arms is escaped, we would predict that the free energy then is

$$\Delta F_{1\text{arm esc}}(H, f)/k_BT = (f - 1)N(H/a)^{-5/3} + R/H \qquad (9)$$

where we have taken eq 5 again to describe the contribution of the escaped arm to the free energy, and the remaining $f - 1$ arms that are still imprisoned yield the same contribution as an imprisoned star with only $f - 1$ arms. However, when eq 9 would hold, the transition between the state with f arms confined (eq 8) and with $(f - 1)$ arms confined (eq 9) would still take place at H_t/a as given by eq 6, i.e., a result independent of f. However, such a result would be at variance with Figure 3. Remember that the escape transitions of the successive arms that leave the region underneath the piston are all strongly rounded, and thus different criteria to locate the transitions give slightly different results, as expected; but the range of H over which the variation of the location of the transition with f changes is much larger than the extent of the rounding.

3. MOLECULAR DYNAMICS SIMULATIONS

We study a coarse-grained model[48] of star polymers with f arms containing $N = 150$ effective monomers each. This model has been studied extensively before, in bulk solution under good solvent conditions[48] and for stars strongly adsorbed on a surface[37] or under confinement in planar slits;[44] hence, we summarize here only a few details of this model. The effective monomers interact with the repulsive part of the (shifted and truncated) Lennard-Jones potentials

$$V(r) = 4\varepsilon[(\sigma/r)^{12} - (\sigma/r)^6 + 1/4], \quad r < r_c = 2^{1/6}\sigma \qquad (10)$$

$V(r > r_c) \equiv 0$, and the strength $\varepsilon \equiv 1$ and range $\sigma \equiv 1$ of this potential are taken as units of temperature and length, respectively. Bonded monomers experience in addition the "FENE potential"[44,45]

$$V_{FENE}(r) = -0.5kr_0^2 \ln[1 - (r/r_0)^2],$$
$$k = 30\varepsilon/\sigma^2, \; r_0 = 1.5\sigma \qquad (11)$$

As usual, molecular dynamics[48,49] simulations are performed, using the velocity-Verlet algorithm to integrate the (Newtonian) equations of motion, to which a friction term plus a random force (related to the friction coefficient by the fluctuation−dissipation relation) is added. Using $m = 1$ as mass for the particles, time is measured in units of $\tau_{MD} = (m\sigma^2/\varepsilon)^{1/2}$, and the integration time step then was taken $0.002\tau_{MD}$ (using a friction coefficient $\gamma = 0.25$). Runs with up to 10^7 MD steps were performed, using typically $f = 6$ and $N = 150$ while the piston radius R and height H above the substrate needed to be varied.

Figure 7 shows typical snapshot pictures for $R = 50$ and several choices of the height H of the piston above the substrate. For $H = 9$ the star typically is still completely imprisoned; for $H = 7$ down to $H = 5.5$, one occasionally observes that one of the arms "tries to escape", but typically there occur a lot of fluctuations, one arm that has escaped retracts again, and another arm escapes. For still smaller H, however, such as $H = 5$ or 4, all arms have escaped already.

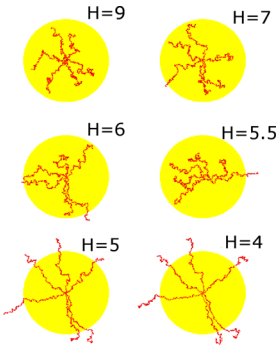

Figure 7. Snapshot pictures of a 6-arm star polymer (top view) with $N = 150$ grafted underneath a piston of radius R = 50 for 6 choices of H, as indicated.

Figure 8a shows the resulting radial monomer density distribution $\rho(r)$, taking all monomers into account. One sees that for small r ($r/\sigma \leq 4$) characteristic oscillations occur,

dx.doi.org/10.1021/ma401356w | Macromolecules XXXX, XXX, XXX−XXX

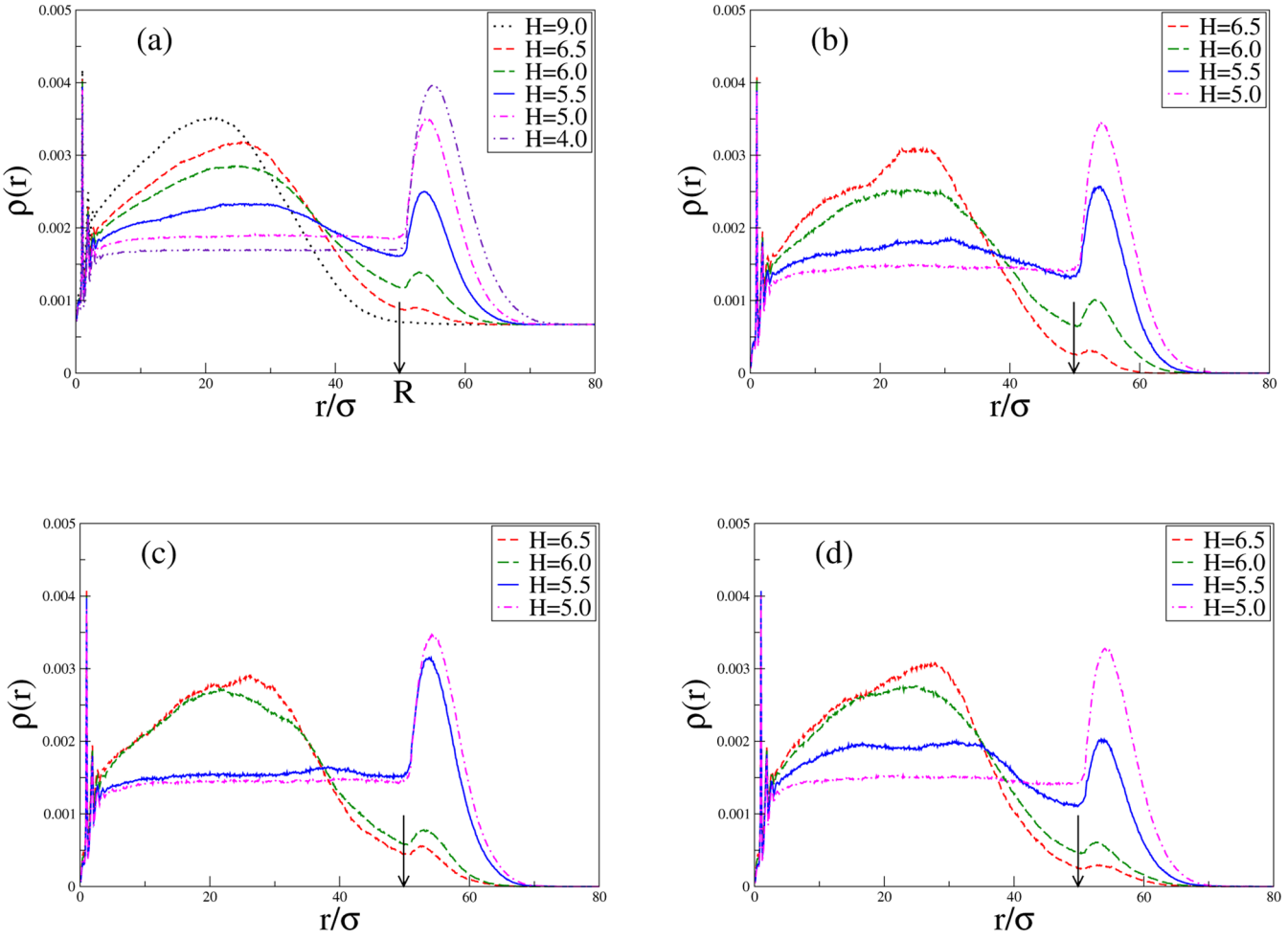

Figure 8. (a) Radial density probability distribution $\rho(r)$ versus dimensionless distance (measured from the grafting point) r/σ, averaged over all 6 arms of a star polymer with $f = 6$ and $N = 150$. Several piston heights H/σ are included as indicated. (b–d) Same as (a), but for the individual arms 1, 3, and 5. The rim of the piston with radius $R = 50$ is indicated by an arrow.

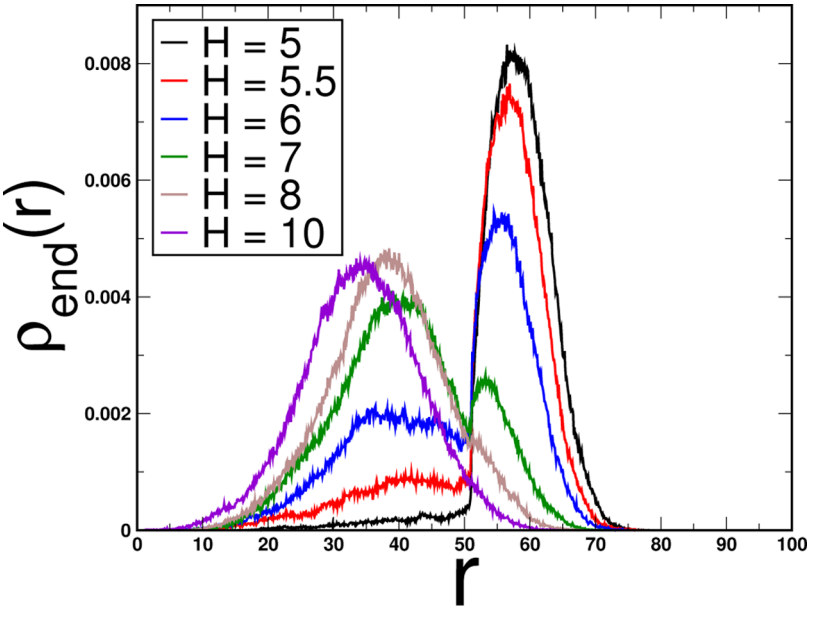

Figure 9. Radial density probability distribution of end-monomers $\rho_{end}(r)$ versus dimensionless distance (measured from the grafting point) r/σ, averaged over all arms of a star polymer with $f = 6$ and $N = 150$. Several piston heights H/σ are included as indicated; the piston radius is $R = 50$.

dx.doi.org/10.1021/ma401356w | *Macromolecules* XXXX, XXX, XXX–XXX

describing a radial layering of the effective monomers around the star center. Of course, this is a model-specific detail, which is of little interest in a scaling context. Apart from this special feature, there is a striking qualitative similarity with the corresponding results of SCF theory (Figure 2b). For H/σ = 9 then ρ (r) exhibits a peak near $r/\sigma \approx 20$. So one would consider this state, in the standard terminology of escape transitions, as an "imprisoned" star, but one should note that a small fraction of monomers is already in the region outside of the piston. For $H/\sigma = 6$ we see already a double peak distribution: the maximum of the escaped part being at $r/\sigma \approx 52$, and the maximum of the "imprisoned" part at $r/\sigma \approx 25$. This maximum clearly is still the dominating one, while for H = 5 the situation has reversed, the maximum representing the escaped part dominates. At very large compression $(H/\sigma = 4)$ the linear variation of $\rho(r)$ with r indicates that the imprisoned part consists just of radially stretched strings of blobs.

The bimodal character of the distribution $\rho(r)$ for intermediate values of H indicates that this escape transition can be viewed as a finite size rounded first-order transition; but clearly the data are insufficient to distinguish a single transition from a series of transitions located close by each other. Figures 8b–d show three typical examples for distributions recorded for single arms (only for H/σ = 5, 5.5, 6, and 6.5). One sees huge fluctuations from arm to arm: some are almost fully escaped in the transition region and some still "imprisoned". Of course, if the running time of the simulation were orders of magnitude larger, all arms would yield an identical distribution. Thus, while the simulations are certainly suggestive of a sequence of transitions, starting with a transition where a single arm escapes, a substantially larger computational effort (hardly feasible at present) would be needed to prove such an arm-by-arm escape.

In Figure 9 we show simulation results for the radial density profiles $\rho_{end}(r)$ of the end-monomers of the star arms (not distinguishing to which arm the ends belong). One sees that for H = 10 and H = 8 the distribution has a single peak at $r = r_{max}^{(1)} < R$ = 50; as H decreases r_{max} increases, as expected. For H = 6 and H = 7, a double-peak structure with two peaks at $r_{max}^{(1)} < R$, $r_{max}^{(2)} > R$ of comparable height is observed, while for H = 5 and H = 5.5 the peak at $r_{max}^{(2)}$ clearly dominates.

Finally, in Figure 10 we display simulation results for the same three observables as shown earlier in Figure 6a for the SCF calculations, i.e., fraction of imprisoned monomers (Figure 10a) and both parallel (Figure 10b) and perpendicular (Figure 10c) components of the squared gyration radius of the grafted star polymer. All three observables are plotted as a function of the piston height H and display the same qualitative behavior as seen earlier in the SCF results shown in Figure 6a.

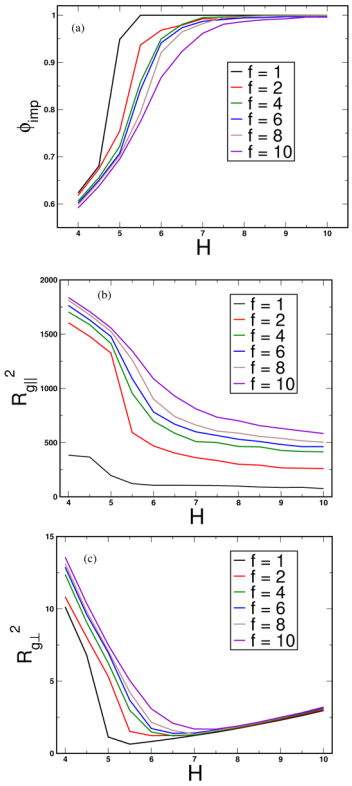

Figure 10. (a) Fraction of imprisoned monomers of the grafted star polymer, plotted vs the piston height H; various numbers of arms f are included, as indicated; all data are for the case R = 50; N = 150. (b) Parallel component of the squared gyration radius vs the piston height H. (c) Perpendicular component of the squared gyration radius vs the piston height H.

4. DISCUSSION AND CONCLUDING REMARKS

In recent years, the effect of chemical architecture of macromolecules (block and graft copolymers, stars, dendrimers, etc.) has become a subject of great interest, since these macromolecules can serve as building blocks of various novel materials. Parallel to this development, the mechanical manipulation of macromolecular objects by external devices (AFM tips, optical and magnetic tweezers) has been developed toward maturity and has yielded a lot of insight into the function of biological molecules grafted to substrates such as biomembranes. In such contexts, it is an interesting variation to consider a grafted star polymer and study its response to mechanical compression, and the escape transition that becomes possible when the mechanical compression acts only over the area of a circle of radius R (Figures 1 and 7), so that some (or all) arms of the star may avoid too strong compression forces by forming a "flower (stem plus crown)" conformation (i.e., a stretched string of blobs extends to the boundary of the piston, so that many monomeric units are in a large "blob", the "crown", outside of the confining piston). While we are not aware that such an experiment already have been performed, we feel that such an experiment should be feasible and could yield interesting insight into the interplay of various entropic forces controlling the conformation of confined macromolecules. Note that instead of an ordinary star polymer one can also graft a spherical polymer brush, containing a (spherical) nanocolloid as a core, to which f long chains (with radii larger than the radius of the nanocolloid) are grafted. We hope that our simulation study will stimulate such experiments.

Using both SCF theory and molecular dynamics simulations, we have shown that for typical choices of parameters the transitions where one arm after the other escapes the confinement are not sharply separated from each other but occur rather gradually (Figures 2, 3, 6, and 10). While the general feature of escape transitions for linear chains and for grafted star polymers are qualitatively similar, the distinctive feature of star polymers is that in the long star limit a sequence of arm-by-arm transitions emerges.

Only when one extracts the coarse-grained free energy functions (Figures 4 and 5) that correspond to configurations constrained such that f_{out} arms are escaped and $f - f_{out}$ arms are not yet escaped, one can verify that in the thermodynamic limit

dx.doi.org/10.1021/ma401356w | Macromolecules XXXX, XXX, XXX–XXX

a sequence of first-order transitions due to arm-by-arm escape will result; for typical choices of parameters, the barriers between the states do not exceed the thermal energy. An interesting extension concerns the competition between adsorption of star polymers and escape when the confining surfaces exhibit an attractive interaction with the monomers. However, this problem must be left for a future study.

While molecular dynamics simulations, in principle, provide exact statistical mechanics for the chosen model system (apart from statistical errors!), the computational effort for parameters of interest is still very large, precluding a systematic variation of all these parameters. Such a variation is considerably easier for the SCF theory: it is well established that the theory works well for dense polymer melts; its accuracy for fairly dilute systems has been rather uncertain. Thus, it is gratifying that for the present problem the simulations reveal a striking qualitative similarity with the SCF results. Of course, a quantitative agreement cannot occur, due to the differences between the lattice model of SCF and continuum model used in the simulations.

AUTHOR INFORMATION

Corresponding Author

*E-mail: paturej@live.unc.edu (J.P.).

Notes

The authors declare no competing financial interest.

ACKNOWLEDGMENTS

A.M. received partial support by the Deutsche Forschungsgemeinschaft (DFG), Grant No. BI 314/23, and S.A.E. received partial support from the Alexander von Humboldt foundation. Computational time on the PL-Grid Infrastructure is gratefully acknowledged.

REFERENCES

(1) Smith, S. B.; Finzi, L.; Bustamante, C. *Science* **1992**, *258*, 1122.
(2) Florin, E. L.; Moy, V. T.; Gaub, H. E. *Science* **1994**, *264*, 415.
(3) Tsckhvretova, L.; Trunck, J.; Sleep, J. A.; Simmons, R. M. *Nature* **1997**, *387*, 308.
(4) Rief, M.; Gautel, M.; Oesterhelt, F.; Fernandez, J. M.; Gaub, H. E. *Science* **1997**, *276*, 1109.
(5) Essevaz-Roulet, B.; Bockelmann, U.; Heslot, F. *Proc. Natl. Acad. Sci. U. S. A.* **1997**, *94*, 11935.
(6) Marszalek, P. E.; Oberhauser, A. F.; Pang, Y. P.; Fernandez, J. M. *Nature* **1998**, *396*, 661.
(7) Mehta, A. D.; Rief, M.; Spudich, J. A.; Smith, R. A.; Simmons, R. M. *Science* **1999**, *283*, 1689.
(8) Mehta, A. D.; Rock, R. S.; Rief, M.; Spudich, J. A.; Mooseker, M. S.; Cheney, R. E. *Nature* **1999**, *400*, 590.
(9) Strick, T. R.; Croquette, V.; Bensimon, D. *Nature* **2000**, *404*, 901.
(10) Kreuzer, H. J.; Grunze, M. *Europhys. Lett.* **2001**, *55*, 640.
(11) Bockelmann, U.; Thomen, Ph.; Essevat-Roulet, B.; Viasnoff, V.; Heslot, F. *Biophys. J.* **2002**, *82*, 1537.
(12) Holland, N. B.; Hugel, T.; Neuert, G.; Oesterhelt, D.; Moroder, L.; Seitz, M.; Gaub, H. E. *Macromolecules* **2003**, *36*, 2015.
(13) Hugel, T.; Rief, M.; Seitz, M.; Gaub, H. E.; Netz, R. R. *Phys. Rev. Lett.* **2005**, *94*, 048301.
(14) Serr, A.; Netz, R. R. *Europhys. Lett.* **2006**, *73*, 202.
(15) Kuhner, F.; Erdmann, M.; Gaub, H. E. *Phys. Rev. Lett.* **2006**, *97*, 21831.
(16) Neuert, G.; Hugel, T.; Netz, R. R.; Gaub, H. E. *Macromolecules* **2006**, *39*, 789.
(17) Strick, T. R.; Dessinges, M.-N.; Charvin, G.; Dekker, N. H.; Allemand, J.-F.; Bennisson, D.; Croquette, V. *Rep. Prog. Phys.* **2003**, *66*, 1.
(18) Klushin, L. I.; Skvortsov, A. M. *J. Phys. A: Math. Theor.* **2011**, *44*, 473001.
(19) Subramanian, G.; Williams, D. R. M.; Pincus, P. A. *Europhys. Lett.* **1995**, *29*, 285.
(20) Subramanian, G.; Williams, D. R. M.; Pincus, P. A. *Macromolecules* **1996**, *29*, 4045.
(21) Williams, D. R. M.; MacKintosh, F. C. *J. Phys. II* **1995**, *5*, 1407.
(22) Gufford, M. C.; Williams, D. R. M.; Sevick, E. M. *Langmuir* **1997**, *13*, 5691.
(23) Jimenez, J.; Rajagopalan, R. *Langmuir* **1998**, *24*, 2598.
(24) Sevick, E. M.; Williams, D. R. M. *Macromolecules* **1999**, *32*, 6841.
(25) Milchev, A.; Yamakov, V.; Binder, K. *Phys. Chem. Chem. Phys.* **1999**, *1*, 2083.
(26) Milchev, A.; Yamakov, V.; Binder, K. *Europhys. Lett.* **1999**, *47*, 675.
(27) Ennis, J.; Sevick, E. M.; Williams, D. R. M. *Phys. Rev.* **1999**, *60*, 6906.
(28) Skvortsov, A. M.; Klushin, L. I.; Leermakers, F. A. M. *Europhys. Lett.* **2002**, *58*, 292.
(29) Klushin, L. I.; Skvortsov, A. M.; Leermakers, F. A. M. *Phys. Rev. E* **2004**, *69*, 061101.
(30) Leermakers, F. A. M.; Skvortsov, A. M.; Klushin, L. I. *J. Stat. Mech.* **2004**, *1*, 10001.
(31) Skvortsov, A. M.; Klushin, L. I.; Leermakers, F. A. M. *J. Chem. Phys.* **2007**, *126*, 024905.
(32) Dimitrov, D. I.; Klushin, L. I.; Skvortsov, A. M.; Milchev, A.; Binder, K. *Eur. Phys. J. E* **2009**, *29*, 9.
(33) De Gennes, P. G. *Scaling Concepts in Polymer Physics*; Cornell University Press: Ithaca, NY, 1979.
(34) Le Guillou, J. C.; Zinn-Justin, J. *Phys. Rev. B* **1980**, *21*, 3976.
(35) Daoud, M.; De Gennes, P. G. *J. Phys. (Paris)* **1977**, *38*, 85.
(36) Grest, G. S.; Fetters, L. J.; Huang, J. S.; Richter, D. *Adv. Chem. Phys.* **1996**, *94*, 67.
(37) Egorov, S. A.; Paturej, J.; Likos, C. N.; Milchev, A. *Macromolecules* **2013**, *46*, 3648.
(38) Likos, C. N.; Harreis, H. M. *Condens. Matter Phys.* **2002**, *5*, 173.
(39) Konieczny, M.; Likos, C. N. *J. Chem. Phys.* **2006**, *124*, 214904.
(40) Konieczny, M.; Likos, C. N. *Soft Matter* **2007**, *3*, 1130.
(41) Halperin, A.; Alexander, S. *Macromolecules* **1987**, *20*, 1146.
(42) Chen, Z.; Escobedo, F. A. *Macromolecules* **2001**, *34*, 8802.
(43) Benhamou, M.; Himmi, M.; Benzouine, F. *J. Chem. Phys.* **2003**, *118*, 4759.
(44) Paturej, J.; Milchev, A.; Egorov, S. A.; Binder, K. *Soft Matter* **2013**, DOI: 10.1039/c3sm51275d.
(45) Sevick, E. M. *Macromolecules* **2000**, *33*, 5743.
(46) Fleer, G. J.; Cohen-Stuart, M. A.; Scheutjens, M. H. J.; Cosgrove, T.; Vincent, B. *Polymers at Interfaces*; Chapman and Hall: London, 1993.
(47) Egorov, S. A. *J. Chem. Phys.* **2011**, *134*, 194901.
(48) Grest, G. S.; Kremer, K.; Witten, T. A. *Macromolecules* **1987**, *20*, 1376.
(49) Grest, G. S.; Kremer, K. *Phys. Rev. A* **1986**, *33*, 3628.